Energy Equip. Sys. / Vol. 8/No. 4/Dec. 2020/ 323-338

ENERGY EQUIPSYS

Energy Equipment and Systems

http://energyequipsys.ut.ac.ir
www.energyequipsys.com

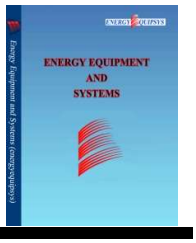

Damping sub-synchronous resonance and improving fault ride through capability: Using S.T.A.T.C.O.M. and S.D.B.R. in a wind power system

Authors

Ehsan Heydari [a]
Ghazanfar Shahgholian [a,b*]

[a] Department of Electrical Engineering, Najafabad Branch, Islamic Azad University, Najafabad, Iran

[b] Smart Microgrid Research Center, Najafabad Branch, Islamic Azad University, Najafabad, Iran

Article history:

Received: 1 September 2019
Accepted: 30 October 2019

ABSTRACT

Concerning wind power penetration into power systems in recent years, the problems of incorrect operation of wind turbines include sub-synchronous resonance (S.S.R.) oscillations and fault ride through (F.R.T.) capabilities need to be fully considered and resolved. In this respect, the S.S.R. phenomenon can severely damage the rotor of an asynchronous generator in a compensated power system with capacitive reactance connected to a wind turbine. Therefore, active and reactive powers of the mentioned systems are controlled by static synchronous compensator (S.T.A.T.C.O.M.) and series dynamic braking resistor (S.D.B.R.); respectively. Moreover, power system designers combine them to improve system stability. In this study, an appropriate method was presented based on the genetic algorithm (G.A.) to provide coordinated and optimal control of STATCOM and S.D.B.R. in order to mitigate S.S.R. and enhance F.R.T. capabilities in a wind farm connected a power system. Optimization variable of this problem included resistance value of S.D.B.R., S.T.A.T.C.O.M. capability, along with its control parameters optimized simultaneously via G.A. to store kinetic energy in the rotor, to control voltage deviations of the wind farm bus, and to minimize speed deviations of the rotor. The proposed method was implemented on the Institute of Electrical and Electronics Engineers (IEEE) first benchmark model to verify the performance of its control structure. The obtained results indicated that coordinated and optimal combination of S.T.A.T.C.O.M. and S.D.B.R. could damp S.S.R. oscillations and augment system stability.

Keywords: Sub-Synchronous Resonance, Fault Ride Through, Optimization, S.D.B.R., S.T.A.T.C.O.M.

1. Introduction

Concerns arising from environmental losses of conventional fossil fuels and growth in energy demands have resulted in increasing use of power production sources such as wind, photovoltaic (P.V.), fuel cells, as well as biomass. In this regard, wind energy, considered as one of the main types of renewable energies, is widespread, dispersed, and decentralized, and accessible at all times in terms of geogr-aphical distribution [1, 2]. The advantages of wind energy include high maneuvering power of utilization (ranging from several watts to several megawatts), no need for fuels in wind turbines, diversity of energy sources, creation of a sustainable energy system, no need for water, as well as absence of environmental pollution [3, 4]. The oscillatory and intermi-

* Corresponding author: Ghazanfar Shahgholian
Department of Electrical Engineering, Najafabad Branch, Islamic Azad University, Najafabad, Iran
Email: shahgholian@iaun.ac.ir

ttent nature of the wind, as well as the capacity of wind turbines to be connected to a network during a fault, are regarded as the inevitable challenges to power systems based on wind farms [5, 6].

The compensation of series capacitors in transmission lines is also taken into account as one of the economical methods to increase transmission power and to improve system stability that can have a significant effect during power transmission [7, 8]. Moreover, there is the problem of sub-synchronous resonance (S.S.R.) in power systems compensated with a series capacitor that receives numerous damages by creating extreme and unstable resonances on the axis of generators [9]. According to the Institute of Electrical and Electronics Engineers (IEEE) benchmark model, S.S.R. represents electrical conditions of power systems. The electrical network and turbo-generator system exchange energy at one or several natural frequencies less than sub-synchronous frequency [10]. Whenever there is a fault, vibrational frequencies are stimulated, and they subsequently exchange energy with electrical resonance frequency [11,12].

Various compensation methods and tools have been further suggested to deal with this problem [13, 14]. For example, in the study conducted by Muyeen, static synchronous compensator (STATCOM) and series dynamic braking resistor (S.D.B.R.) were simultaneously used to augment fault ride through (F.R.T.) as well as transient stability of wind farms [15]. Accordingly, the results of simulation in different kinds of faults indicated enhanced F.R.T. and transient stability in comparison with the status wherein S.T.A.T.C.O.M. and S.D.B.R. had been separately used. In the other investigation completed by Mahfouz et al., there were attempts to investigate the implementation of three-level inverters based on S.T.A.T.C.O.M. to improve F.R.T. and stability of fixed-speed wind farms [16].

The main challenge of implementing the suggested method was determining an optimal capacity for S.T.A.T.C.O.M. In the aforementioned study, a simple method was also provided to evaluate S.T.A.T.C.O.M. capacity for regulating the point of common coupling voltage level. The related simulation was conducted under different fault conditions, and the findings revealed augmented low-voltage ride-through (L.V.R.T.) and F.R.T. via installing S.T.A.T.C.O.M. In their investigation, Daoud et al. also provided a reliable structure for the transmission system of voltage source converter/high-voltage direct current (VSC-HVDC) of offshore wind farms and seaside networks [17]. Thanks to its power distribution balance, a flywheel energy storage system (FESS) could work in their study as the wave power absorber during a fault. As the cycle of these waves was relatively short, it was observed that the FESS could reduce this problem in an effective manner. Another application of FESS included improved F.R.T. during the fault and enhanced performance of power levels in working conditions.

Furthermore, the findings indicated the efficiency of the suggested structure to fulfill the intended purposes. In this respect, a flexible F.R.T. mechanism for a power system with high-wind power penetration was investigated in the study by Wang et al. [18]. This mechanism included requirements of adaptive F.R.T. and maximum power limitation of wind farms with low F.R.T. capabilities. The requirements related to the capacity of adaptive F.R.T. in the suggested mechanism involved ride through sub-scale faults and a transient L.V.R.T. (related to sub-scale and medium scale faults). The simulation results suggested that the flexible F.R.T. mechanism had increased the F.R.T. capability of wind farm clusters and mitigated wind power oscillations during the fault. In the study by Rashid et al., bridge-type fault current limiter (B.F.C.L.) had been similarly used to enhance the F.R.T. capabilities of fixed-speed wind generators [19]. To investigate the efficiency and superiority of this method, a comparison had also been made with the results of the dynamic braking resistor (D.B.R.), and the findings had demonstrated that use of B.F.C.L. could have a significant effect on enhancing F.R.T. capabilities of wind turbines and reducing harmonics to a significant level. In the end, it had been indicated that B.F.C.L. had been

much better than a resistor in the transmission circuit.

Moreover, a static volt-ampere reactive (V.A.R.) compensator (S.V.C.) and S.T.A.T.C.O.M. had been used in the investigation by Pereira et al. (2014) to maintain the stability of wind turbines under fault conditions [20]. Given the limitations of reactive power generation in the network, two parallel compensators had been employed in their method. Moreover, flexible alternating current transmission system (FACTS) devices had been used to control reactive power in the network and to improve voltage stability conditions [21]. In the study conducted by Hossain et al. (2010), S.T.A.T.C.O.M. together with its coordinated control with the controller of generator pitch angle had been used [22], indicating that the mechanical structure of wind turbines could have a significant effect on turbine stability, and instability would occur if it were ignored. Thus, in the aforementioned study, S.T.A.T.C.O.M. control had been simultaneously conducted with pitch angle control.

To mitigate S.S.R., various devices have been so far used, including S.V.C. [23], distributed static series compensator (D.S.S.C.) [24], unified power flow controller (U.P.F.C.) [25], as well as thyristor controlled series capacitor (T.C.S.C.) [26]. In the study by Prasad et al., fuzzy logic had been used to control S.T.A.T.C.O.M. [27]. In an investigation by Raju et al., the fractional-order proportional integral (F.O.P.I.) controller had been applied to control the structure of the united power flow distribution [28]. Moreover, the Kalman filter had been employed for S.T.A.T.C.O.M. in the study by Rajaram et al. [29]. There had also been attempts in the investigation conducted by Adrees et al. to use optimal compensation of transmission lines to minimize S.S.R. risks [30]. In the study by Carpanen et al. [31], S.T.A.T.C.O.M. had also been applied. Additionally, Ghorbani et al. employing a sub-synchronous damping controller (S.S.D.C.) along with S.T.A.T.C.O.M. [32] had indicated the desired performance of this controller in S.S.R. damping. In the study by Khazaie et al., D.S.S.C. had been utilized with a conventional damping controller (C.D.C.) based on particle swarm optimization (PSO) and fuzzy logic based damping controller (F.L.B.D.C.) to reduce S.S.R. These simulations had suggested better performance of F.L.B.D.C. in terms of mitigating S.S.R. [33].

Following the penetration of wind energy sources into power systems, it is of utmost importance to investigate the effect of wind turbines on S.S.R. oscillations and F.R.T. capabilities. Once wind turbines are connected to a power system compensated with series capacitor, numerous damages occur to the rotor of synchronous generators. In this respect, S.T.A.T.C.O.M. and S.D.B.R. have the ability to control reactive and active powers, and their combination is also assumed as a desired method to improve stability. In the present study, S.S.R. and F.R.T. capabilities were simultaneously applied, and a new method was provided for coordinated and optimal control of STATCOM and S.B.D.R. to reduce S.S.R. oscillations and to augment F.R.T. capabilities. To achieve a resistant control, a G.A. was suggested for optimizing the capacity of S.T.A.T.C.O.M. and S.D.B.R. aimed to minimize the kinetic energy saved in the rotor, change the bus voltage connected to the wind farm, and control speed deviations of the rotor. To create a single-purpose function, a maximum geometric mean formulation was also applied. The results of the simulation also indicated that the given method not only had improved F.R.T. capabilities but also had a high capacity in damping S.S.R. oscillations. In comparison with the studies conducted by Muyeen (2015) and Ghorbani et al. (2012), the advantages of the present study included high convergence power and algorithm speed used as well as simultaneous improvement of S.S.R. and F.R.T. capabilities.

2. Sub-synchronous resonance

S.S.R. is known as a phenomenon related to energy exchange between the mechanical system of a turbo generator and an electrical system. Some parts of a turbo-generator are also fluctuating at some frequencies, known as torsional vibrations, which are determined based on mechanical features such as hardness, mass, and inertia of different components of the axis. Whenever the system

frequency is by 60 hertz, the frequency of these vibrations can range from 10 to 55 hertz [34, 35]. The natural frequency of resonance for electrical systems is also equal to [36]:

$$\omega_e = \frac{1}{\sqrt{L_T C}} = \frac{\omega_0}{\sqrt{(\omega_0 L_T)(\omega_0 C)}} = \omega_0 \sqrt{\frac{X_C}{X_{LT}}} \quad (1)$$

$$f_e = f_0 \sqrt{\frac{X_C}{X_{LT}}}, \quad (2)$$

In which f_o is the synchronous frequency of the system ($\omega_o=2\pi f_o$, $f_o=60HZ$), X_c shows capacitor reactance of transmission line, and $X_{L.T.}$ stands for inductive reactance of the entire electrical system comprised of the sub-transient reactance of the generator ($X^{''}G$), transformer reactance ($X_{T.}$), and inductive reactance of the transmission line (X_{line}). Given the compensation level of the transmission line, that is commonly less than 100%; f_e is less than f_o according to resonance frequency equation. Therefore, f_e frequency is referred to as the natural sub-synchronous frequency of the electrical system. The mutual pitch also includes both electrical and mechanical systems. When sub-synchronous frequency of the voltage component inducted in the armature is close to or equal to that of the electrical resonance, the resulted sub-synchronous flow can lead to torque production in the rotor that will subsequently bring about rotor vibrations and consequently strengthens rotor torque that causes rotor wear and damage. The vibrations of the rotor in the generator at pitch frequency of f_m will also result in the induction of voltage components with f_{em} frequency in the stator. The frequency of f_{em} is equal to:

$$f_{em} = f_0 \pm f_m \quad (3)$$

3. Model and control structure of the case study

Figure 1 illustrates the investigated system and simulation analysis. In this structure, G1 and G2 synchronous generators are connected through T1 and T2 transformers, respectively. Moreover, the compensated transmission line is connected to a wind farm consisting of 20 wind generators via a series capacitor. The information related to the parameters of G1 and G2 synchronous generators had been respectively provided in the studies by Muyeen et al. [2008] and Farmer [1985]. To access the information related to the transmission line and the multi-mass axis parameters of the G2 turbine generator, the information obtained from Farmer's study was used. G2 generator axis has also been designed as a 6-mass model [Fig. 2]. The information of the axis multi-mass model of the generator can be found in the studies conducted by Muyeen et al. [37], Farmer [38], and Papathanassiou et al. [39].

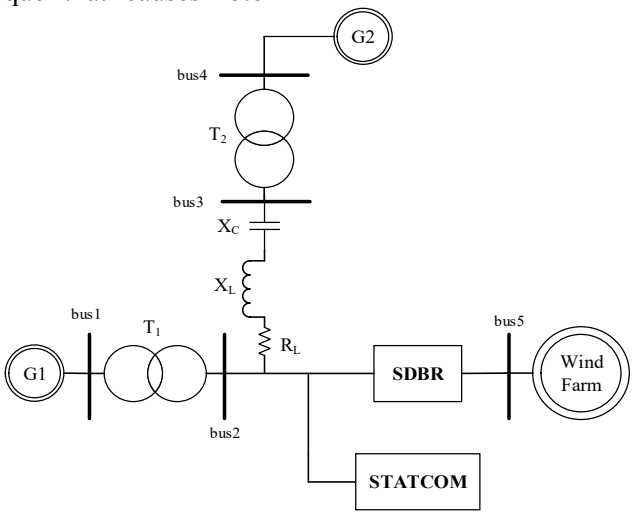

Fig. 1. Power system under study

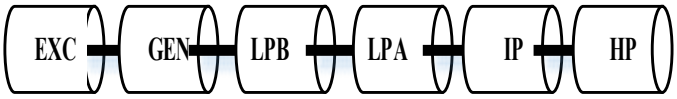

Fig. 2. Six-mass drive train model

In the present study, a coordinated controlling schema has been developed for S.T.A.T.C.O.M. and S.D.B.R. to damp the vibrations of the system under fault conditions [Fig. 3]. Accordingly, S.D.B.R. improves F.R.T. capability and reduces vibration range through recovering the terminal voltage of the wind farm. Moreover, STATCOM damps the vibrations existing in the system by providing reactive power. Under fault conditions, the terminal voltage of the farm mitigates all of a sudden. In this status, the $V_{.W.F.}$ terminal voltage of the wind farm is compared with the reference voltage of V_{ref} that is 0.9. If $V_{.W.F.}$ terminal voltage is more than V_{ref}, signal 1 is sent, and S.D.B.R. of the connection is reduced. Otherwise, signal 0 is sent to S.D.B.R., so that the resistor is placed in the circuit. The S.D.B.R. consists of three keys paralleled with three static resistors whose related details are provided in Fig. 4.

[1] The control structure of S.T.A.T.C.O.M. has been indicated in Fig. 5. In this structure, voltage conversion angle changes from the three-phase voltages ($V_{.A.}$, $V_{.B.}$, $V_{.C.}$) to d-q axis ones through applying phase-locked loop (P.L.L.). The voltage-supported converter can be thus controlled by using four proportional integral (P.I.) controllers. The first P.I. controller is PI-1, used for creating the reverence valued axis current ($I_{d\text{-}ref}$), applying the difference between the real value and the reference one of D.C. link voltage. Comparing the reference and the real value of d axis current (I_d), the obtained result is used as the input signal of the third P.I. controller (PI-3).

[2] Then, the reference value of d axis voltage ($V_{d\text{-}ref}$) results as the output signal of this controller.

Likewise, the second P.I. controller (PI-2) is employed for creating the reference value of q axis current ($I_{q\text{-}ref}$) from the difference existing between the real value of bus2 voltage (V_{bus2}) and the reference value of bus2 voltage ($V_{bus2\text{-}ref}$). Comparing the reference value of the q axis current ($I_{q\text{-}ref}$) with the real value of the q axis current (I_q), the obtained result is utilized as the input signal of the fourth P.I. controller (PI-4).

Then, the reference value of d axis voltage ($V_{q\text{-}ref}$) results as the output signal of this controller. Both $V_{d\text{-}ref}$ and $V_{q\text{-}ref}$ are correspondingly converted to three-phase reference voltages ($V_{A,\ B.C\text{-}ref}$) by using voltage conversion angle through P.L.L. Comparing $V_{A,\ B.C\text{-}ref}$ with a wave containing a triangle with the frequency of 1980 hertz, the fault signal enters the space vector modulation for producing stimulation signals of the inverter. This block has the responsibility of producing six stimulation signals for the voltage source of a three-leg inverter. As observed, PI-1, PI-2, PI-3, and PI-4 controllers are respectively used with the capability of regulating their gains to remove the difference existing among the measured values with the nominal ones of V_{dc}, V_{bus2}, I_d, and I_q.

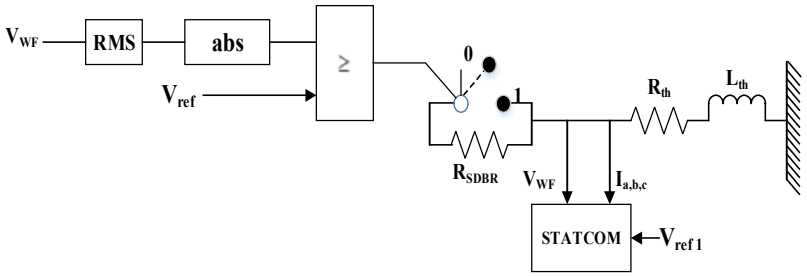

Fig. 3. Proposed coordinated control scheme for system stability

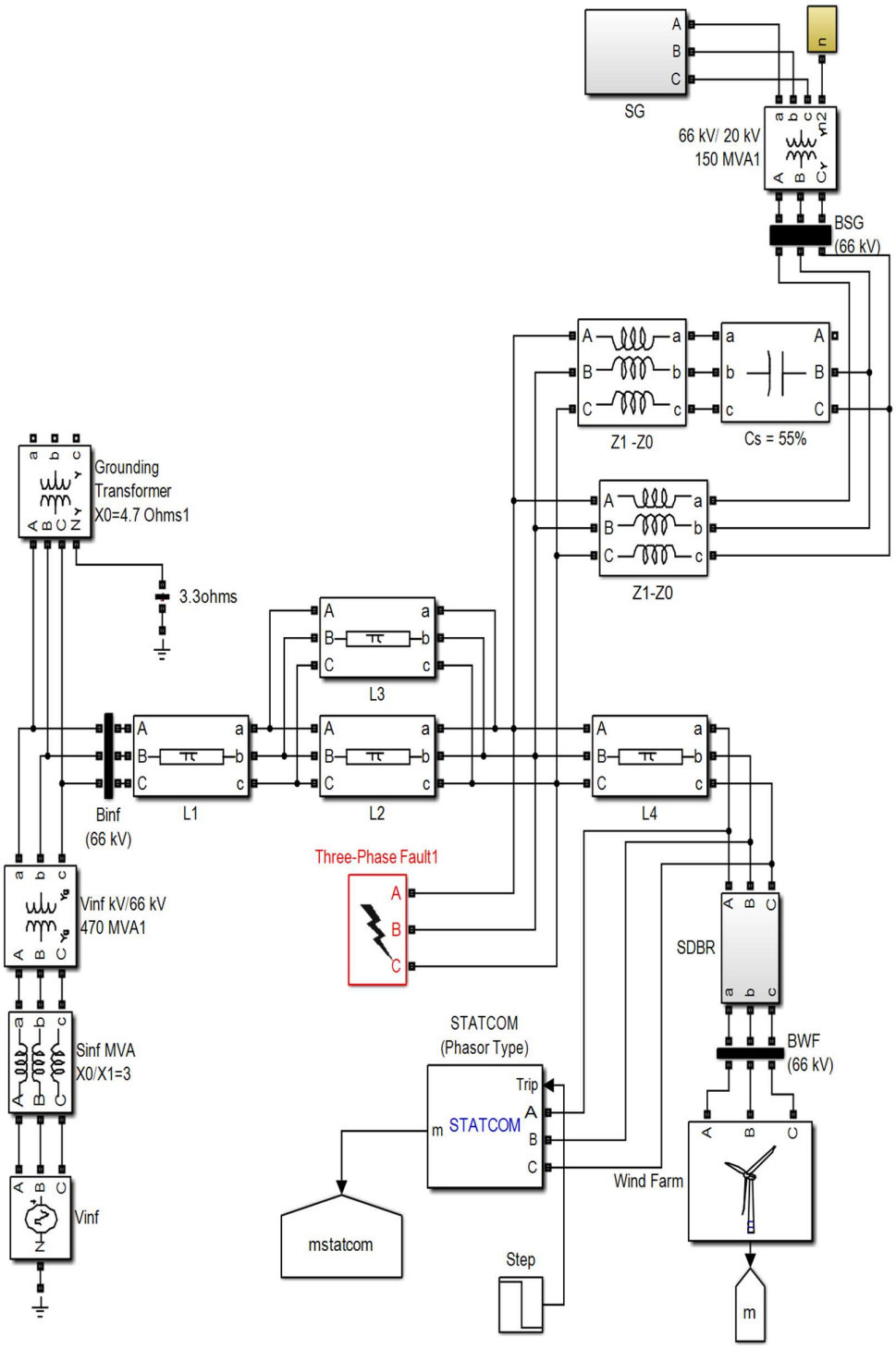

Fig. 4. Control structure of S.D.B.R.

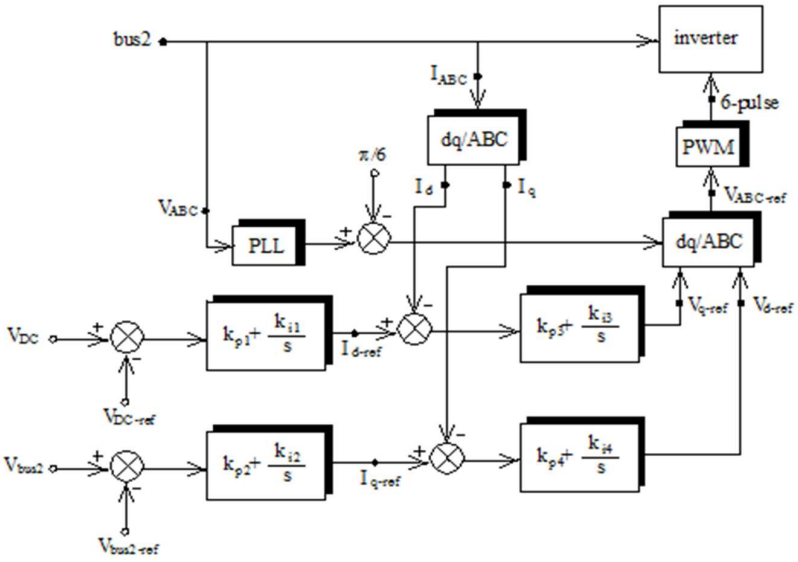

Fig. 5. Control block diagram of S.T.A.T.C.O.M.

4. Proposed Optimization Method

As indicated, the purpose/functions consider the changes of bus voltage of wind farms and speed deviation of the rotor through minimizing the kinetic energy saved in the rotor.

The optimization variables include S.D.B.R. resistance (R_{opt}), STATCOM capacity (S_{opt}), A.C. voltage regulator gains (K_{p1}, K_{i1}), D.C. voltage (K_{p2}, K_{i1}), as well as S.T.A.T.C.O.M. current (K_{p1}, K_{i1}, K_f). The purpose/functions are elaborated in the following sections.

4.1. Stored Kinetic Energy in Rotor

The first vibrations of rotor angle and rotor speed are minimized once the kinetic energy saved ($E_{K.E.}$) in the rotor is minimized at the fault incidence time, expressed as [40]:

$$E_k^f = A\left(t_c - t_o\right)^2 , \tag{4}$$

where parameter A is described as

$$A = \frac{1}{2} M \alpha^2 , \tag{5}$$

in which M is the fixed inertia of synchronous generator rotor, to refers to fault incidence time, tc shows fault removal time, and α stands for acceleration time of the rotor at the fault incidence time. The estimated α is measured as:

$$\alpha = \frac{\left(P_m - P_{ef}\right)}{M} , \tag{6}$$

where P_m and P_{ef} are, respectively, generator input mechanical power and output electrical power at the fault incidence time. Thus, parameter A defined as

$$f_1 = A = \frac{1}{2M}\left(P_m - P_{ef}\right)^2 , \tag{7}$$

is minimized instead of reducing the kinetic energy saved:

4.2. Speed Deviations of Rotor

The speed deviation of the G2 generator rotor is defined by using the absolute value integral relation of fault in time using [41]:

$$f_2 = ITAE = \int_0^\infty t\left|\omega(t)\right| dt . \tag{8}$$

4.3. Voltage Deviations of Wind Farm Terminal

The terminal voltage changes of wind farms are described by using the absolute value integral index in time. That is

$$f_3 = ITAE = \int_0^\infty t\left|1 - V_{WF}\right| dt . \tag{9}$$

4.4. Multi-Objective Formulation

The maximum geometric mean formulation for creating a multi-purpose function is given as [42]:

$$F_{tot} = \left(f_1 \times f_2 \times f_3\right)^{1/3} \quad . \tag{10}$$

4.5. Constraints of Problem

Since the present study primarily focuses on the optimal regulation of S.D.B.R. resistance, S.T.A.T.C.O.M. capacity, alternating current (A.C.) vs. Direct current (D.C.) (AC-DC) voltage controlling parameters, and S.T.A.T.C.O.M. current; the limitations of the problem include high and low ranges of these parameters defined as follows [15]:

$$\begin{aligned} &0.001 \le R_{opt} \le 1 \\ &5 \le S_{opt} \le 40 \\ &1 \le k_{p1} \le 10,\ 500 \le k_{i1} \le 1100 \\ &0.00001 \le k_{p2} \le 0.001,\ 0.01 \le k_{i2} \le 0.1 \\ &0.1 \le k_{p3} \le 1,\ 1 \le k_{i3} \le 15,\ 0.1 \le k_f \le 1 \end{aligned} \tag{11}$$

4.6. Genetic Algorithm

To minimize the function of the main purpose, as indicated in relation (10), the genetic algorithm G.A. was used. The problem-solving flowchart of G.A. is presented in Fig. 6.

5. Simulation Results

In this section, a temporary three-phase fault occurs at t=1.1 s for 150 ms. Input parameters of G.A. are shown in Table 1. By applying G.A., optimal values along with those of the target function are listed in Table 2. Using GA on optimization objective function in (10), convergence curve is shown in Fig. 7.

Applying GA in the 10th iteration is depicted in Figs. 8-15. S.S.R. is also investigated through Figs. 8, 9 and 10, while improved stability and F.R.T. are discussed in Figs. 10-15.

However, both non-optimal and proposed method in [32] are compared in Figs. 8-10 for validating the efficiency of the suggested method. For this purpose, speed deviation of G1 generator ($\Delta\omega_1$), low-voltage part ($\Delta\omega_2$), and high-voltage part ($\Delta\omega3$) are shown in Fig.11.

In addition, the generator axis, the torque between different parts of the generator and the low-voltage turbine torque (T1), and the torque between different parts of the low-voltage turbine and the high-voltage turbine of the generator axis (T2) are provided in Fig.12, respectively.

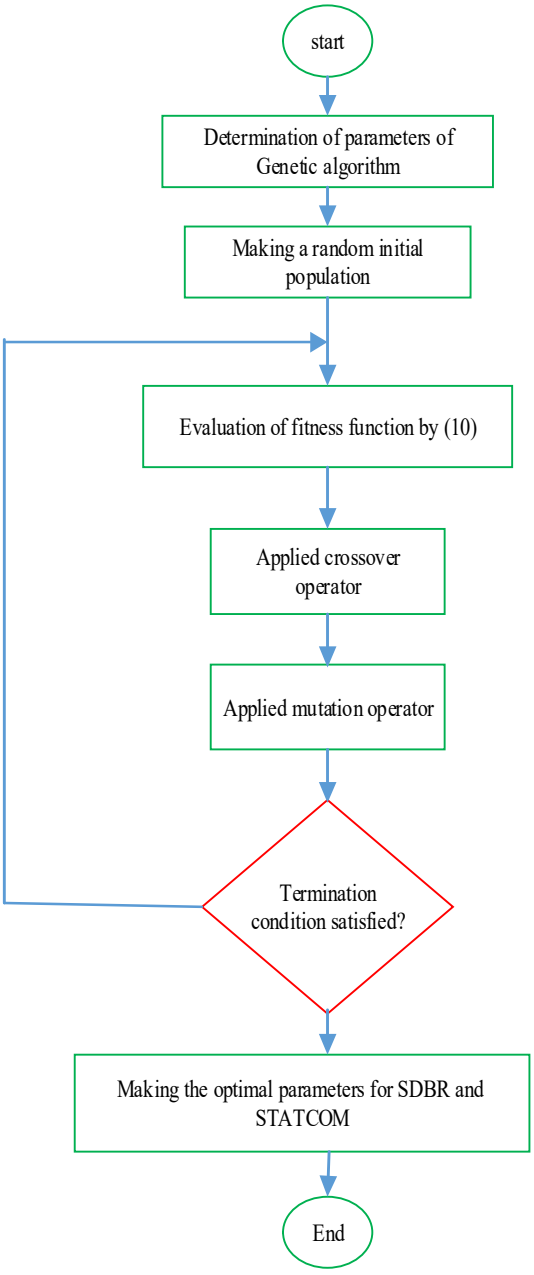

Fig. 6. Genetic algorithm problem-solving flowchart

Table 1. G.A. parameters

Parameter	Value
Population size	20
Iterations	20
Mutation probability	0.3
Crossover probability	0.7

Table 2. Optimal parameters derived from G.A.

Parameter	value
R_{opt}(pu)	0.79241
S_{opt}(M.W.)	39.59492
k_{p1}, k_{i1}	6.90166,907.1423
k_{p2}, k_{i2}	0.00085,0.04735
k_{p1}, k_{p2}, k_{p3}	0.37149,11.6083,0.39725
f_1, f_2, f_3	0.00341,0.1381,0.0871

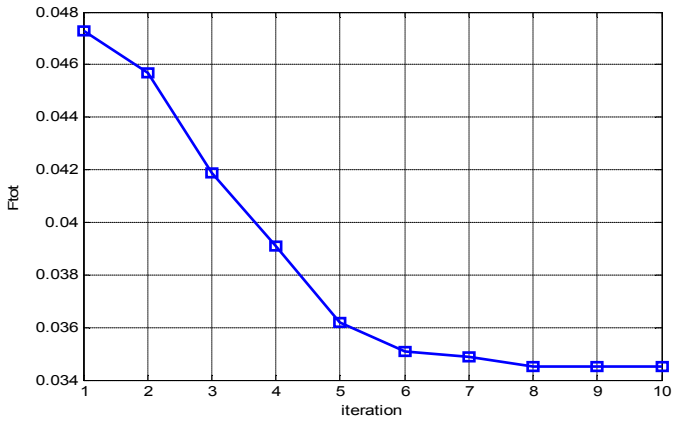

Fig. 7. Convergence curve of the multi-objective function using G.A.

Clearly, the presented optimization is more effective than other methods in terms of damping and improving S.S.R. vibrations. In order to confirm the effectiveness of the optimal S.T.A.T.C.O.M. and S.D.B.R. in augmenting system stability and F.R.T. capabilities, both suggested methods [15] are compared with the optimal method in Figs. 13, 14 and 15. For this purpose, Figs. 10-15 indicate the terminal voltage of wind farms ($V_{W.F.}$), electromagnetic torque, load angle of G1 generator, as well as active and reactive powers of G2 generator, respectively. Once the fault occurs, the terminal voltage of wind farms is suddenly decreased.

Furthermore, the electromagnetic torque, load angle, and active and reactive powers associated with numerous fluctuations are damped after removing the fault. As can be seen, upon the application of optimal S.D.B.R. and S.T.A.T.C.O.M., the drop of terminal voltage reduces, and its changes are kept at the minimum possible level in comparison with the reference value. The vibrations of electromagnetic torque, generator load angle, and active and reactive powers of the G2 generator also mitigate at the fault incidence time, and consequently, F.R.T. and stability of the system are improved. As observed, the vibrations of electromagnetic torque, generator load angle, and active and reactive powers of G2 generator are reduced at the fault incidence time, and the F.R.T. and stability are subsequently enhanced through adopting the suggested method.

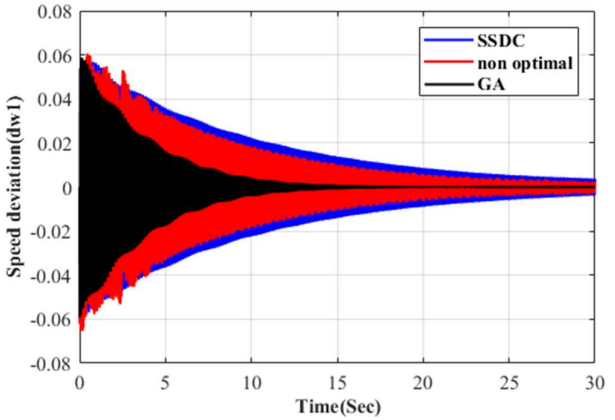

(a) $\Delta\omega_1$

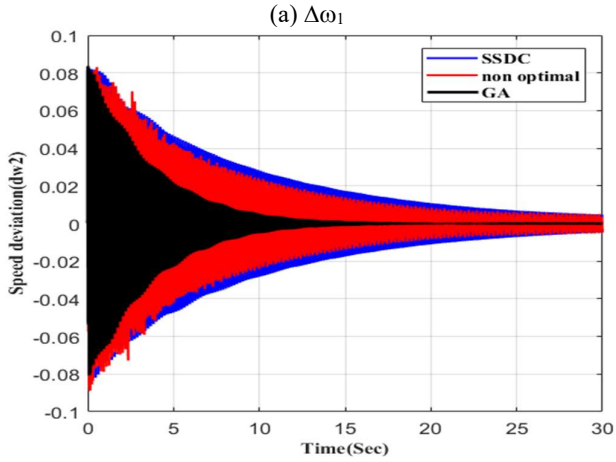

(b) $\Delta\omega_2$

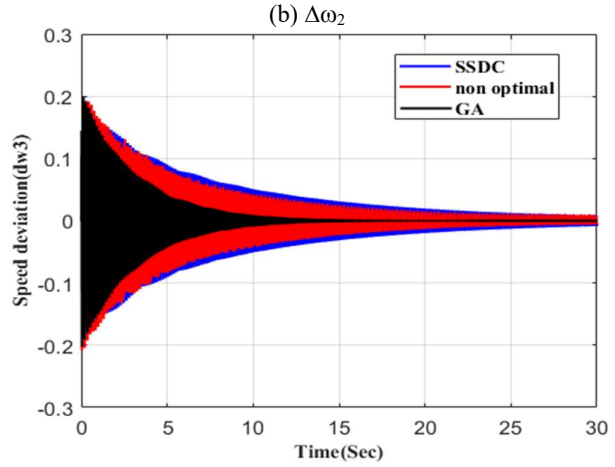

(c) $\Delta\omega_3$

Fig. 8. Damping of generator vibrations in speed deviation in the presence of S.T.A.T.C.O.M. and S.D.B.R.

Comparing the findings of the present study with those reported by Muyeen et al. (2015), it can be concluded that the structure suggested by the present study is more efficient than that of the aforementioned study in terms of damping vibrations and providing a stable response.

Despite the responses related to electro-magnetic torque, generator load angle, and active and reactive powers of G2 generator; it can be concluded that the existing vibrations are damped very quickly, and also the speed of reaching complete stability is higher in the method suggested in the present study.

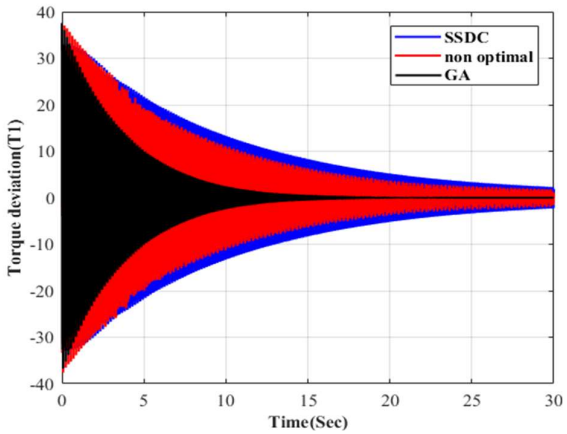

Fig. 9. Damping of torque vibrations in the presence of S.T.A.T.C.O.M. and S.D.B.R. between generator parts and low-voltage turbines (T1)

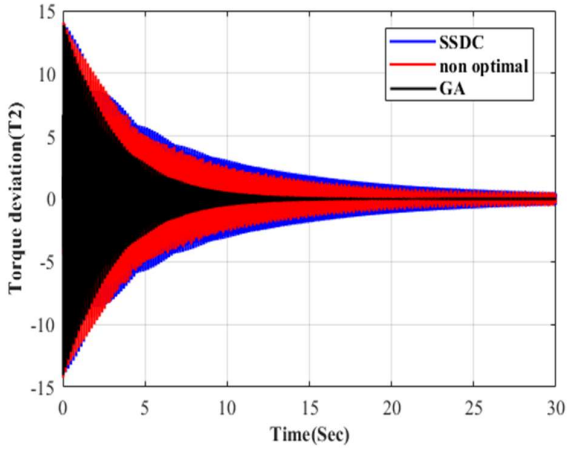

Fig. 10. Damping of torque vibrations in the presence of S.T.A.T.C.O.M. and S.D.B.R. (b) between different parts of low-voltage and high-voltage turbines (T2)

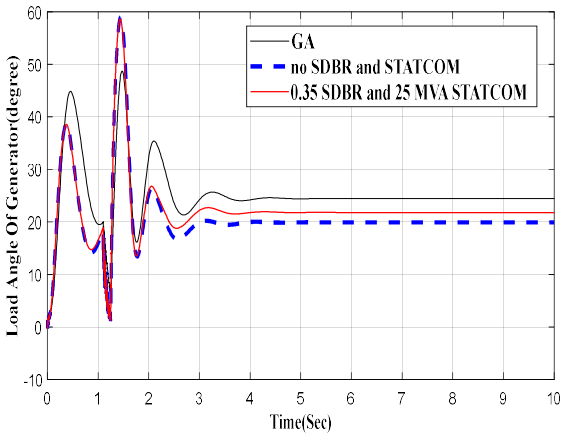

Fig. 11. Damping of vibrations created in the presence of S.T.A.T.C.O.M. and S.D.B.R. in load angle of G2 generator

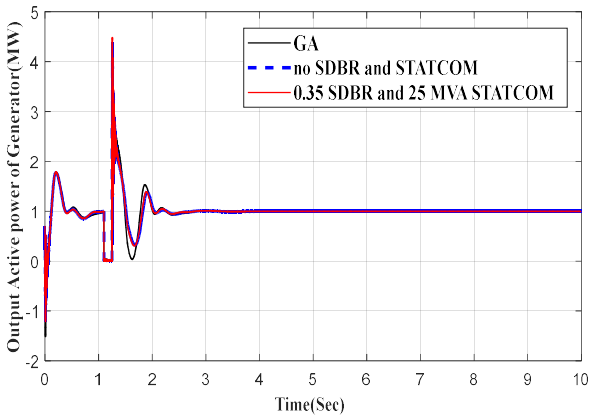

Fig. 12. Damping of vibrations created in the presence of S.T.A.T.C.O.M. and S.D.B.R. in G2 generator output active power

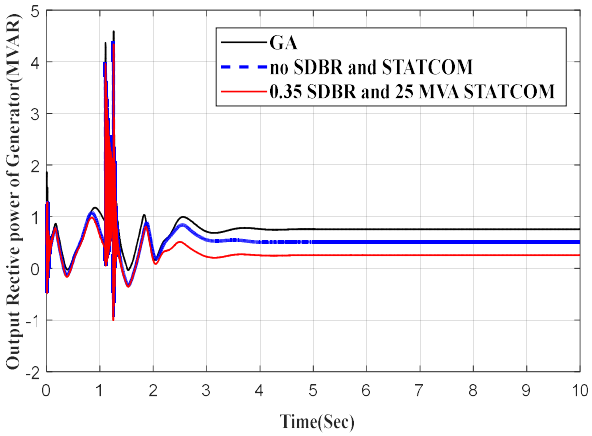

Fig. 13. Damping of vibrations created in the presence of S.T.A.T.C.O.M. and S.D.B.R. in G2 generator output reactive power

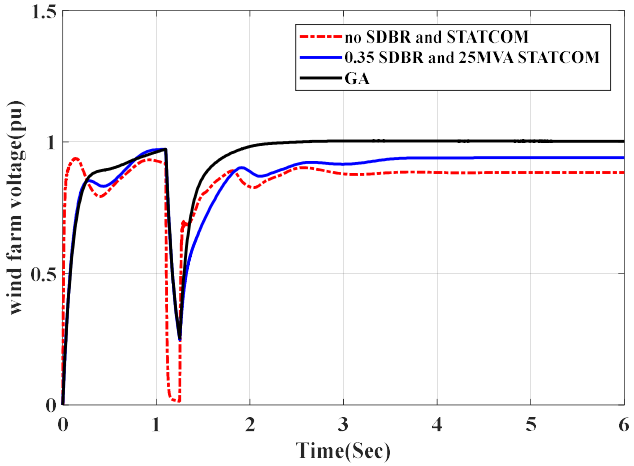

Fig. 14. The terminal voltage of wind farms ($V_{W.F.}$) in the presence of S.T.A.T.C.O.M. and S.D.B.R.

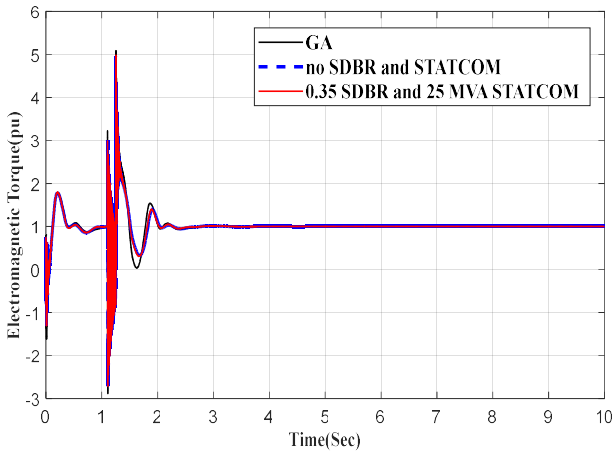

Fig. 15. Electromagnetic torque in the presence of S.T.A.T.C.O.M. and S.D.B.R.

6. Conclusion

In the present study, the coordinated and optimal control of S.T.A.T.C.O.M. and S.D.B.R. is suggested for damping the S.S.R. oscillations of a transmission line compensated with series capacitor and improving F.R.T. capabilities. To this end, optimization was formulated as a multi-purpose problem, and S.T.A.T.C.O.M. and S.D.B.R. optimal parameters were determined using G.A. to minimize the multi-purpose function. The simulation results obtained indicated high efficiency of the suggested method in terms of damping S.S.R. oscillations and improving F.R.T. capabilities. To provide a numerical comparison between the optimal mode of the proposed system and its non-optimal mode, the values of S.T.A.T.C.O.M and S.D.B.R. parameters could be taken into account. In the non-optimal mode, the STATCOM and S.D.B.R. values were 25 M.V.A. and 0.35 pu; respectively. In the optimal mode, the S.T.A.T.C.O.-M. and S.D.B.R. values were 39.59492 MVA and 0.79241 pu, respectively.

References

[1] E. Abbaspour, B. Fani and E. Heydarian-Forushani, “A bi-level multi agent based protection scheme for distribution networks with distributed generation”, International Journal of Electrical Power and Energy Systems, Vol. 112, pp. 209-220, 2019.

[2] G. Shahgholian and Z. Azimi, "Analysis and design of a DSTATCOM based on sliding mode control strategy for improvement of voltage sag in distribution systems", Electronics, Vol. 5, No. 3, pp. 1-12, 2016.

[3] M. Mahdavian and N. Behzadfar, “A review of wind energy conversion system and application of various induction generators”, Journal of Novel Researches on Electrical Power, Vol. 8, No. 4, pp. 55-66, 2020.

[4] M. Tavoosi, B. Fani and E. Adib, “Stability analysis and control of DFIG based wind turbine using FBC strategy”, Journal of Intelligent Procedures in Electrical Technology, Vol. 4, No. 15, pp. 31-42, 2013.

[5] H. A. Mohammadpour and E. Santi, “S.S.R. damping controller design and optimal placement in rotor-side and grid-side converters of series-compensated DFIG-based wind farm”, IEEE Trans. on Sustainable Energy, Vol. 6, No. 2, pp. 388-399, 2015.

[6] G. Shahgholian, K. Khani and M. Moazzami, "Frequency control in autanamous microgrid in the presence of DFIG based wind turbine", Journal of Intelligent Procedures in Electrical Technology, Vol. 6, No. 23, pp. 3-12, 2015.

[7] X. Xie, H. Liu and Y. Han, “Coordinated design of supplementary excitation damping controller and voltage-sourced converter based generator terminal subsynchronous damping controller for

subsynchronous resonance suppression: A case study", Electric Power Components and Systems, Vol. 44, No. 5, pp. 565-577, 2016.

[8] E. Barocio, P. Zuniga, S. Vazquez and R. Betancourt, "Simplified recursive Newton-type algorithm for instantaneous modal parameter estimation of sub-synchronous oscillations", Electric Power Components and Systems, Vol. 40, No. 8, pp. 864-880, 2012.

[9] Y. Wang, Q. Wu, R. Yang, G. Tao and Z. Liu, "H_∞ current damping control of D.F.I.G. based wind farm for subsynchronous control interaction mitigation", International Journal of Electrical Power and Energy Systems, Vol. 98, pp. 509-519, 2018.

[10] A. Shoulaie, M. Bayati-Poudeh, G. Shahgholian, "Damping torsional torques in turbine-generator shaft by novel PSS based on genetic algorithm and fuzzy logic", Journal of Intelligent Procedures in Electrical Technology, vol. 1, no. 2, pp. 3-10, Summer 2010.

[11] I.S.R.W. Group, "Proposed terms and definitions for subsynchronous oscillations", IEEE Trans. on Power Apparatus and Systems, Vol. 99, No. 2, pp. 506-511, 1980.

[12] V.B. Virulkar and G.V. Gotmare, "Subsynchronous resonance in series compensated wind farm: A review", Renewable and Sustainable Energy Reviews, Vol. 55, pp. 1010–1029, March 2016.

[13] W. Du, X. Wang and H. Wang, "Subsynchronous interactions caused by the P.L.L. in the grid-connected P.M.S.G. for the wind power generation", International Journal of Electrical Power and Energy Systems, Vol. 98, pp. 331-341, 2018.

[14] A.Q. Al-Shetwi, M.Z. Sujod, F. Blaabjerg, Y. Yang, "Fault ride-through control of grid-connected photovoltaic power plants: A review", Solar Energy, Vol. 180, pp. 340-350, March 2019,

[15] S. Muyeen, "A combined approach of using an S.D.B.R. and a S.T.A.T.C.O.M. to enhance the stability of a wind farm", IEEE Systems Journal, Vol. 9, No. 3, pp. 922-932, 2015.

[16] M. Mahfouz and M. A. El-Sayed, "Static synchronous compensator sizing for enhancement of fault ride-through capability and voltage stabilisation of fixed speed wind farms", I.E.T. Renewable Power Generation, Vol. 8, No. 1, pp. 1-9, 2014.

[17] M.I. Daoud, A.M. Massoud, A.S. Abdel-Khalik, A. Elserougi, and S. Ahmed, "A flywheel energy storage system for fault ride through support of grid-connected VSC HVDC-based offshore wind farms", IEEE Trans. on Power Systems, Vol. 31, No. 3, pp. 1671-1680, 2016.

[18] S. Wang et al., "Flexible fault ride through strategy for wind farm clusters in power systems with high wind power penetration", Energy Conversion and Management, Vol. 93, pp. 239-248, 2015.

[19] G. Rashid and M.H. Ali, "A modified bridge-type fault current limiter for fault ride-through capacity enhancement of fixed speed wind generator", IEEE Trans. on Energy Conversion, Vol. 29, No. 2, pp. 527-534, 2014.

[20] R.M. Pereira, C.M. Ferreira, and F.M. Barbosa, "Comparative study of S.T.A.T.C.O.M. and S.V.C. performance on dynamic voltage collapse of an electric power system with wind generation", IEEE Latin America Trans., Vol. 12, No. 2, pp. 138-145, 2014.

[21] G. Shahgholian and N. Izadpanahi, "Improving the performance of wind turbine equipped with DFIG using STATCOM based on input-output feedback linearization controller", Energy Equipment and Systems, Vol. 4, No. 1, pp. 65-79, 2016.

[22] M.J. Hossain, H.R. Pota, V.A. Ugrinovskii, and R.A. Ramos, "Simultaneous S.T.A.T.C.O.M. and pitch angle control for improved L.V.R.T. capability of fixed-speed wind turbines," IEEE Trans. on sustainable energy, Vol. 1, No. 3, pp. 142-151, 2010.

[23] F.C. Jusan, S. Gomes, and G.N. Taranto, "S.S.R. results obtained with a dynamic phasor model of S.V.C. using modal analysis", International Journal of

Electrical Power and Energy Systems, Vol. 32, No. 6, pp. 571-582, 2010.

[24] Z. Amini Khouei and A. Kargar, "Reduction of Sub-synchronous Resonances with D-FACTS Devices using intelligent Control", Journal of Intelligent Procedures in Electrical Technology, Vol. 7, No. 26, pp. 3-14, 2017.

[25] S. Golshannavaz, F. Aminifar, and D. Nazarpour, "Application of U.P.F.C. to enhancing oscillatory response of series-compensated wind farm integrations", IEEE Trans. on Smart Grid, Vol. 5, No. 4, pp. 1961-1968, 2014.

[26] P. Vuorenpää and P. Järventausta, "Effect of generic synchronization approaches on subsynchronous damping characteristics of thyristor controlled series capacitor", I.F.A.C. Proceedings Volumes, Vol. 42, No. 9, pp. 404-409, 2009.

[27] C. E. Prasad and S. Vadhera, "Fuzzy logic based S.S.S.C. as sub- synchronous resonance damping controller", Proceeding of the IEEE/ICEPE, pp. 1-4, Shillong, India, June 2015.

[28] D.K. Raju, B.S. Umre, A.S. Junghare, and B.C. Babu, "Mitigation of subsynchronous resonance with fractional-order P.I. based U.P.F.C. controller," Mechanical Systems and Signal Processing, Vol. 85, pp. 698-715, 2017.

[29] T. Rajaram, J. M. Reddy, and Y. Xu, "Kalman filter based detection and mitigation of subsynchronous resonance with S.S.S.C.", IEEE Trans. on Power Systems, Vol. 32, No. 2, pp. 1400-1409, 2017.

[30] A. Adrees and J. V. Milanović, "Optimal compensation of transmission lines based on minimisation of the risk of subsynchronous resonance", IEEE Trans. on Power Systems, Vol. 31, No. 2, pp. 1038-1047, 2016.

[31] R. P. Carpanen and B. Rigby, "A contribution to modelling and analysis of SSSC-based power flow controls and their impact on S.S.R.", Electric Power Systems Research, Vol. 88, pp. 98-111, 2012.

[32] A. Ghorbani, B. Mozaffari, and A. Ranjbar, "Application of subsynchronous damping controller (S.S.D.C.) to S.T.A.T.C.O.M.", International Journal of Electrical Power and Energy Systems, Vol. 43, No. 1, pp. 418-426, 2012.

[33] J. Khazaie, M. Mokhtari, M. Khalilyan, and D. Nazarpour, "Sub-synchronous resonance damping using distributed static series compensator (D.S.S.C.) enhanced with fuzzy logic controller", International Journal of Electrical Power and Energy Systems, Vol. 43, No. 1, pp. 80-89, 2012.

[34] R. Farmer, A. Schwalb, and E. Katz, "Navajo project report on subsynchronous resonance analysis and solutions", IEEE Trans. on Power Apparatus and Systems, Vol. 96, No. 4, pp. 1226-1232, 1977.

[35] P. Li, L. Xiong, F. Wu, M. Ma, J. Wang, "Sliding mode controller based on feedback linearization for damping of sub-synchronous control interaction in DFIG-based wind power plants", International Journal of Electrical Power & Energy Systems, Vol. 107, pp. 239-250, May 2019,

[36] P. Kundur, N. J. Balu, and M. G. Lauby, Power system stability and control. McGraw-Hill, New York, 1994.

[37] S. Muyeen, J. Tamura, and T. Murata, Stability augmentation of a grid-connected wind farm, Springer Science and Business Media, 2008.

[38] R. Farmer, "Second benchmark model for computer simulation of subsynchronous resonance IEEE subsynchronous resonance working group of the dynamic system performance subcommittee power system engineering committee", IEEE Power Engineering Review, No. 5, pp. 34-34, 1985.

[39] S. A. Papathanassiou and M. P. Papadopoulos, "Mechanical stresses in fixed-speed wind turbines due to network disturbances", IEEE Trans. on Energy Conversion, Vol. 16, No. 4, pp. 361-367, 2001.

[40] I. Ngamroo and T. Karaipoom, "Cooperative control of S.F.C.L. and S.M.E.S. for enhancing fault ride-through capability and smoothing power fluctuation of D.F.I.G. wind farm", IEEE Trans. on

Applied Superconductivity, Vol. 24, No. 5, pp. 1-4, 2014.

[41] S. Panda, A. Baliarsingh, S. Mahapatra, and S. Swain, "Supplementary damping controller design for S.S.S.C. to mitigate sub-synchronous resonance", Mechanical Systems and Signal Processing, Vol. 68, pp. 523-535, 2016.

[42] R. Vince, "The leverage space trading model: Reconciling portfolio management strategies and economic theory", Wiley Publishing, 2015.